

RCS2D: A 2D Scattering Simulator for MoM vs. FDTD Comparisons

Gizem Toroğlu¹, Mehmet Alper Uslu¹, and Levent Sevgi^{1,2}

¹ Electronics and Communications Engineering Department
Doğuş University, 34722 Istanbul – Turkey
torogluzem@yahoo.com, alperuslu@ieee.org

² Electrical and Computer Engineering Department
University of Massachusetts, Lowell, MA – USA
lsevgi@dogus.edu.tr, Levent_sevgi@uml.edu

Abstract – A Java-based, two dimensional (2D) electromagnetic wave scattering and Radar Cross-Section (RCS) simulation software, RCS2D Virtual Tool, is developed. Both Method of Moments (MoM) and Finite-Difference Time-Domain (FDTD) methods are used to simulate the Transverse Magnetic (TM) and Transverse Electric (TE) polarized scattering waves for arbitrary geometries and materials under the plane wave illumination.

Index Terms - Electromagnetic waves, FDTD, MoM, radar cross section (RCS), scattering, TM, and TE.

I. INTRODUCTION

Electromagnetic (EM) scattering deals with wave and object interaction. Understanding this interaction and scattering is essential in low-visible target design, cancer detection, mine exploration, etc. A Java-based, two dimensional (2D) simulator (i.e., RCS2D) is developed for the investigation of EM scattering from arbitrary objects and different materials. First version of the simulator was presented in [1]. In this paper, the latest version, which can handle arbitrary EM materials, is introduced.

The simulator deals with geometries shown in Fig. 1. Here, an infinitely long, either conducting or dielectric/ferrite cylinder with user-drawn arbitrary cross section located along the z-axis and illuminated by a plane wave from a specified direction is taken into account. The simulations are

performed with two powerful numerical models (MoM and FDTD), which make comparisons possible. The TM and TE problems are both investigated.

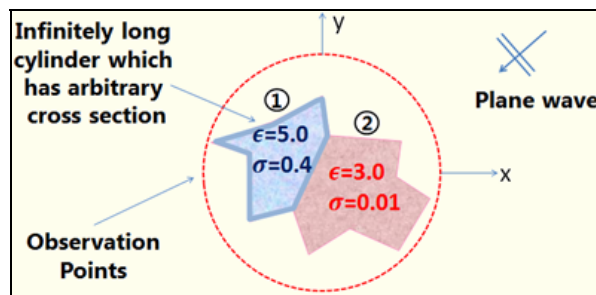


Fig. 1. An object with arbitrary cross section illuminated by a plane wave from a given direction.

II. THE METHOD OF MOMENTS (MOM) MODEL

MoM is a frequency domain model and has been in use since 1960s [2] (see, also [3] for a tutorially review of MoM and some simple applications). It is based on the discretization/reduction of time-harmonic EM field integral equations into a linear matrix system. MoM model for dielectric cylinders of arbitrary cross section was first proposed by Richmond in [4] and then generalized to dielectric / diamagnetic objects with oblique incident case in [5]. Although, both TM_z and TE_z polarizations are implemented only TM_z equations are included here.

The incident field components for the TM_z case are in the form of,

$$E_z^{(inc)} = E_0 e^{jk_0(x(n)\cos(\phi)+y(n)\sin(\phi))} \quad (1)$$

$$H_x^{(inc)} = \frac{E_0 k_0 \sin(\phi)}{\mu\omega} E_z^{(inc)}, \quad (2)$$

$$H_y^{(inc)} = -\frac{E_0 k_0 \cos(\phi)}{\mu\omega} E_z^{(inc)},$$

where ϕ is the incident angle, k_0 is the free space wave number, E_0 is the amplitude of the incident electric field, and N is the total number of cells ($n=1,2,\dots,N$). After calculating the incident fields, a size of $3N \times 1$, Y matrix is constructed as,

$$Y = \begin{bmatrix} E_z^{(inc)} & \eta_0 H_x^{(inc)} & \eta_0 H_y^{(inc)} \end{bmatrix}^T \quad (3)$$

where η_0 is the free space wave impedance.

The incident fields create surface currents on the surface of the object and that currents then produce scattered fields. The total field is the sum of incident and scattered fields,

$$\begin{aligned} E_z &= E_z^{inc} + E_z^s \\ H_x &= H_x^{inc} + H_x^s, \\ H_y &= H_y^{inc} + H_y^s. \end{aligned} \quad (4)$$

The cross section of the object under investigation is divided into small pieces (compared to wavelength) called segments (or patches). The problem is discretized accordingly and a matrix form is obtained,

$$[Z] \begin{bmatrix} E_z & \eta_0 H_x & \eta_0 H_y \end{bmatrix}^T = Y. \quad (5)$$

The $3N \times 3N$, Z matrix shown in equation (5) is expressed as follows,

$$Z = \begin{bmatrix} A & B & C \\ D & E & F \\ G & F & H \end{bmatrix} \quad (6)$$

and the entries of the Z matrix are given in Table 1. Here, $a_{m,n}$ is the area of the rectangular cell at the location of m or n , $\mu_{r(m,n)}$ is the relative magnetic permeability of the m^{th} or n^{th} cell and $\epsilon_{r(m,n)}$ is the relative electric permittivity of the m^{th} or n^{th} cell. Electric field of each cell can be calculated from equation (5),

$$\begin{bmatrix} E_z & \eta_0 H_x & \eta_0 H_y \end{bmatrix}^T = [Z]^{-1} \begin{bmatrix} E_z^{(inc)} & \eta_0 H_x^{(inc)} & \eta_0 H_y^{(inc)} \end{bmatrix}^T. \quad (7)$$

The electric field component of the scattered field at any point outside the dielectric body is given by,

$$\begin{aligned} E_z^s &= j \frac{\pi}{2} \sqrt{\frac{2j}{\pi}} \sum_{n=1}^N k a_n J_1(k a_n) e^{jk(x_n \cos \phi + y_n \sin \phi)} \frac{e^{-jk\rho_0}}{\sqrt{k\rho_0}} \times \\ &\quad [(\mu_m - 1)[\eta_0 H_{yn} \cos \phi - \eta_0 H_{xn} \sin \phi]]. \end{aligned} \quad (8)$$

Scattered fields of the observation angle ϕ can be represented in terms of RCS (σ) defined as,

$$\begin{aligned} W(\phi) &= \lim_{\rho_0 \rightarrow \infty} 2\pi\rho_0 \left| \frac{E_z^s(\rho_0, \phi)}{E_z^i} \right|^2 \\ W(\phi) &= \frac{\pi^2 k}{|E^i|^2} \left| \sum_{n=1}^N (\epsilon_n - 1) E_{zn} a_n J_1(k a_n) e^{jk(x_n \cos \phi + y_n \sin \phi)} \right|^2. \end{aligned} \quad (9)$$

III. THE FINITE DIFFERENCE TIME DOMAIN (FDTD) MODEL

The FDTD model, first proposed by K. S. Yee in 1966 [6], which is based on the application of second-order center difference approach to time and spatial derivatives in Maxwell's equations. FDTD is a time domain method and frequency domain responses are extracted by using Fourier Transform (FT). Due to its finite nature, original Yee algorithm should be modified at the terminals of the simulation space. In addition, near-to-far field (NTFF) transformation is required to handle RCS problems. The time domain NTFF transforms give broadband frequency response and are useful for mono-static RCS simulations. The frequency domain NTFF transformations give direct (discrete) frequency response but useful for bi-static RCS simulations. Both transformations utilize surface equivalence theorem on a virtual closed surface placed at a particular distance. The far field response is then calculated via these surface currents. In RCS2D, free-space effects are simulated via perfectly matched layer (PML) approach and the frequency domain NTFF transformation is used [7].

VI. THE RCS2D VIRTUAL TOOL AND EXAMPLES

The front panel graphical user interface (GUI) of the java-based RCS2D virtual tool is illustrated in Fig. 2. It has two distinct EM solvers (MoM and FDTD). The virtual tool can run with both models and results may be compared in terms of accuracy and computation time.

Table 1: The entries of the Z matrix.

$m \neq n$	$m = n$
$A_{mn} = -(\epsilon_m - 1) \frac{\pi k a_n}{2j} J_1(k a_n) H_0^{(2)}(k \rho_{mn})$	$A_{mmm} = 1 + \frac{j}{2} (\epsilon_m - 1) [\pi k a_m H_1^{(2)}(k a_m) - 2j]$
$B_{mn} = \frac{\pi k a_n}{2} J_1(k a_n) (\mu_m - 1) (y_m - y_n) \frac{H_1^{(2)}(k \rho_{mn})}{\rho_{mn}}$	$B_{mmm} = 0$
$C_{mn} = -\frac{\pi k a_n}{2} J_1(k a_n) (\mu_m - 1) (x_m - x_n) \frac{H_1^{(2)}(k \rho_{mn})}{\rho_{mn}}$	$C_{mmm} = 0$
$D_{mn} = \frac{\pi k a_n}{2} J_1(k a_n) (\epsilon_m - 1) (y_m - y_n) \frac{H_1^{(2)}(k \rho_{mn})}{\rho_{mn}}$	$D_{mmm} = 0$
$E_{mn} = \frac{(\mu_m - 1) \pi j k a_n}{2} J_1(K a_n) \frac{-1}{(k \rho_{mn})^3} \times$ $\left[-k^3 \rho_{mn} (y_m - y_n)^2 H_0^{(2)}(k \rho_{mn}) \right.$ $\left. + [(y_m - y_n)^2 - (x_m - x_n)^2] k^2 H_1^{(2)}(k \rho_{mn}) \right]$	$E_{mmm} = 1 + \frac{j(\mu_m - 1)}{4} [\pi k a_m H_1^{(2)}(k a_m) - 4j]$
$F_{mn} = -\frac{(\mu_m - 1) \pi k a_n J_1(k a_n) k^2}{2j (k \rho_{mn})^3} (x_m - x_n) (y_m - y_n) \times$ $[2H_1^{(2)}(k \rho_{mn}) - k \rho_{mn} H_0^{(2)}(k \rho_{mn})]$	$F_{mmm} = 0$
$G_{mn} = \frac{-\pi k a_n}{2} J_1(k a_n) (\epsilon_m - 1) (x_m - x_n) \frac{H_1^{(2)}(k \rho_{mn})}{\rho_{mn}}$	$G_{mmm} = 0$
$H_{mn} = 1 + \frac{j(\mu_m - 1)}{4} [\pi k a_m H_1^{(2)}(k a_m) - 4j]$	$H_{mmm} = \frac{(\mu_m - 1) \pi j k a_n}{2} J_1(K a_n) \frac{1}{(k \rho_{mn})^3}$ $\left[-k^3 \rho_{mn} (x_m - x_n)^2 H_0^{(2)}(k \rho_{mn}) \right.$ $\left. + [(x_m - x_n)^2 - (y_m - y_n)^2] k^2 H_1^{(2)}(k \rho_{mn}) \right]$

Highly effective charts are included; thus, the visualization of the simulation results becomes attractive. The front panel is split into four subsections. The top block contains numerous image buttons to improve accessibility. The left block is divided into two: collapsible workspace and summary subpanels. Workspace demonstrates all features that are supplied by the program. The summary part provides the user to observe all actions as well as computer resources. The right panel has four tabs: simulation area, model, visualization, and simulation results. The user draws any object/geometry he or she desires via the simulation area tab. The model tab shows the segmentation of the objects. The visualization tab is reserved for real-time wave monitoring of FDTD based simulations. Simulation results tab is reserved for the polar plots.

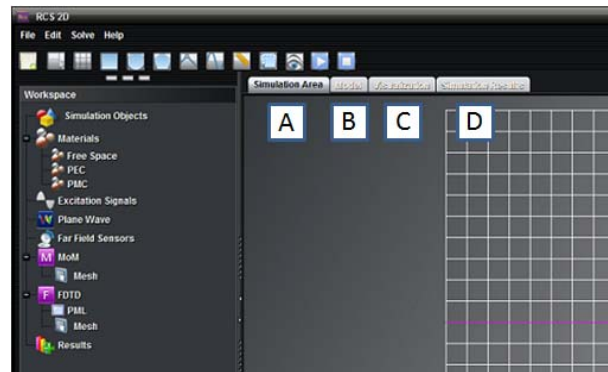


Fig. 2. Front panel of the RCS2D (A: simulation area, B: model, C: visualization, and D: simulation results).

The program provides three basic geometric buttons (square, ellipse, and polygon) to make object creation/drawing easy. Scaling, translating,

rotating, and mirroring the objects is possible. Object dragging is also included. Overlapping objects (after dragging or rotating, etc.) are categorized according to the user decision.

Several tests with different materials and geometries are performed to illustrate the power of the RCS2D tool and comparisons are given below. MoM and FDTD models are also validated through these tests. First, an infinite cylinder with the cross section shown in Fig. 3 (a) is taken into account. The dimensions and the frequency are given in the figure inset. The cylinder is formed of two lossy dielectric parts. This cylinder is illuminated by a plane wave from an angle of 30° and bi-static scattered fields are recorded all around. The observation points are located at 4 m away. Results for the TM_z polarization are given in Fig. 3 (b). As observed, forward scattered field is dominant and MoM and FDTD results agree very well.

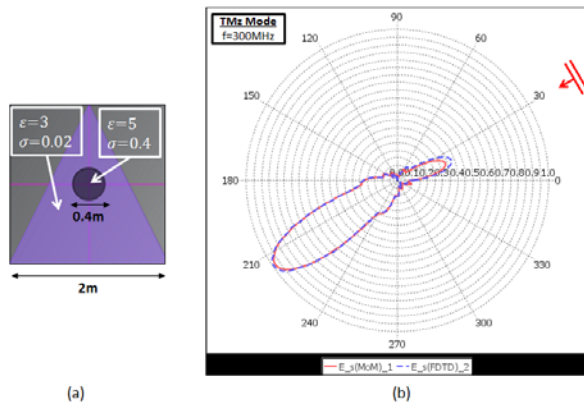


Fig. 3. (a) The first test cylinder and (b) the scattered field of the test cylinder.

The second example belongs to the RCS of another inhomogeneous dielectric object. The cross section of the object used in this example is shown in Fig. 4 (a). The cylinder is composed of two lossy dielectric triangles and the illuminated angle of the incident plane wave is 240° . The results for the same polarization are shown in Fig. 4 (b).

The third example belongs to an F-shaped dielectric infinite cylinder and again the TM_z mode. The object is illuminated by a plane wave having an incident angle of 330° . The results are given in Fig. 5.

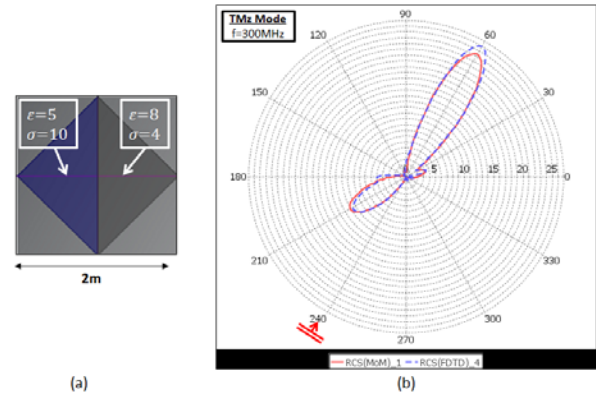


Fig. 4. (a) The second test cylinder and (b) the RCS of the test cylinder.

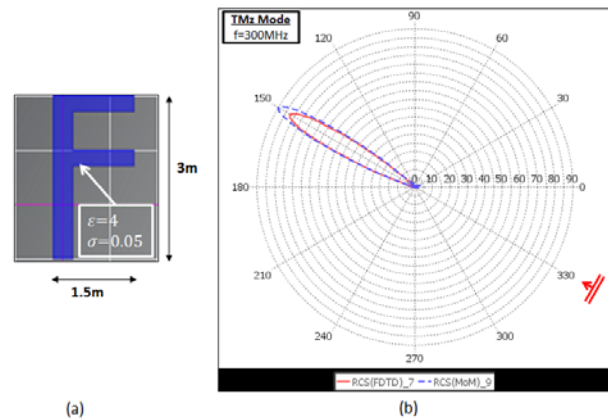
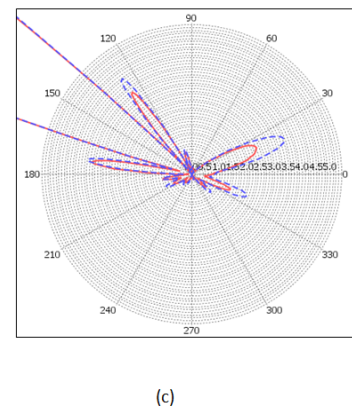


Fig. 5. (a) An F-shaped lossy dielectric cylinder, (b) RCS vs. angle, and (c) magnified view.



The final example investigates an infinite lossy dielectric square cylinder for the TE_z case. The size of a square is 0.4 m. The frequency is 600 MHz. The angle of the incident plane wave is 30° and observation points are located on a circle enclosing the object with 5 m radius. Figure 6 (a)

shows the structure and the scattered fields are given in Fig. 6 (b).

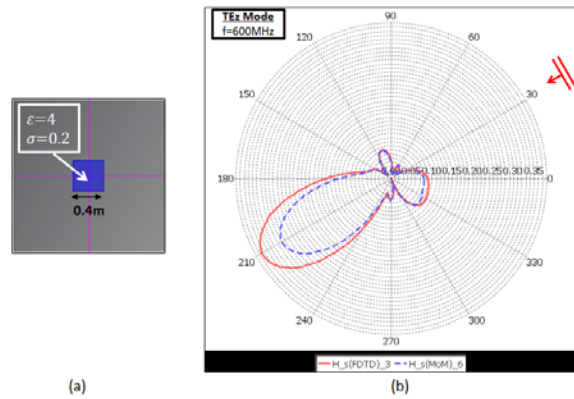


Fig. 6. (a) A square shaped lossy dielectric cylinder and (b) the scattered field of the test cylinder at 5 m away.

Any object can be modeled in RCS2D by specifying conductivity, permittivity, and permeability. PEC objects can also be modeled by giving significantly high conductivities. Note that, rough discretization is used for both MoM and FDTD calculations to speed up the computations. This is one of the reasons of discrepancies between MoM and FDTD results in the plots (another reason is the incapability of diffraction modeling in MoM). Better agreement will be obtained if object discretization is performed with a higher number of cells/segments. FDTD requires much more memory, but is much faster when compared to MoM.

V. CONCLUSION

An attractive EM scattering simulation package (RCS2D) is presented. Method of Moments (MoM) and Finite-Difference Time-Domain (FDTD) method are used to simulate both TM and TE polarized scattered fields. EM scattering of arbitrary geometries and different materials under plane wave illumination can be investigated with RCS2D.

REFERENCES

- [1] G. Toroglu, A. Uslu, and L. Sevgi, "RCS2D: A 2D MoM and FDTD based simulator", *MMS 2012, The 12th Mediterranean Microwave Symposium*, Dogus University, Istanbul, Turkey, Sep. 14-16, 2012.
- [2] [3] R. F. Harrington, *Field Computation by Moment Method*, New York: IEEE Press, (First Ed. 1968), 1993.
- [3] E. Arvas and L. Sevgi, "A tutorial on the method of moments," *IEEE Antennas and Propagation Magazine*, vol. 54, no. 3, pp. 260-275, June 2012.
- [4] J. H. Richmond, "TE-wave scattering by a dielectric cylinder of arbitrary cross-section shape," *IEEE Trans. Antennas Propagat.*, vol. 14, no. 4, pp. 460-464, 1966.
- [5] R. G. Rojas, "TE-wave scattering by a dielectric cylinder of arbitrary cross-section shape," *IEEE Trans. Antennas Propagat.*, vol. 36, no. 2, pp. 238-246, 1988.
- [6] K. S. Yee, "Numerical solution of initial boundary value problems involving Maxwell's equations in isotropic media," *IEEE Trans. Antennas and Propagat.*, vol. 14, pp. 302-307, 1966.
- [7] J. P. Berenger, "Three dimensional perfectly matched layer for the absorption of electromagnetic waves," *Journal of Computational Physics*, vol. 127, pp. 363-379, 1996.